Relaxation from a marginal state in optical bistability

P. Colet and M. San Miguel
Departamento de Física, Universitat de les Illes Balears, E-07071 Palma de Mallorca, Spain

J. Casademunt and J. M. Sancho
Departamento d'Estructura i Constituents de la Matèria, Universitat de Barcelona, Diagonal 647, E-08028 Barcelona, Spain
(Received 28 July 1988)

Characteristic decay times for relaxation close to the marginal point of optical bistability are studied. A model-independent formula for the decay time is given which interpolates between Kramers time for activated decay and a deterministic relaxation time. This formula gives the decay time as a universal scaling function of the parameter which measures deviation from marginality. The standard deviation of the first-passage-time distribution is found to vary linearly with the decay time, close to a marginality, with a slope independent of the noise intensity. Our results are substantiated by numerical simulations and their experimental relevance is pointed out.

I. INTRODUCTION

Consider a dynamical system which can be described by a potential for a single relevant degree of freedom. A state of marginal stability is then defined as an inflection stationary point of the potential. The order of the first nonvanishing derivative of the potential classifies the order of different possible marginal states. We consider here the marginal state of lowest order. A characteristic example of this type of marginal state appears at the end points (spinodal points) of a hysteresis cycle. In the case of optical bistability (OB) the output intensity presents a hysteresis cycle when plotted versus the intensity of the driving laser. The end point of the hysteresis cycle occurs for a certain value of the incident intensity. For this value of the parameter the dynamics is determined by a potential which has a marginal state. The marginal state is the point at which the unstable and locally stable branches coalesce. The normal form of the potential associated with a marginality of this type is given by

$$V(x)=-ax^3+bx^4-\beta x, \quad a,b>0 . \tag{1.1}$$

The marginal state occurs for $\beta=0$ at $x=0$. The saturation term bx^4 gives global stability (see Fig. 1). In optical bistability β is the difference between the incident intensity and its value at the end point of the hysteresis circle. The driving force for $\beta=0$ vanishes at the marginal state and it drives the system to $x=0$ or away from $x=0$ for small deviations to the left and right of the origin, respectively. In this sense the marginal state has mixed characteristics of a locally stable ($x<0$) and locally unstable state ($x>0$).

Relaxation from marginal states has several interesting features that make it different from relaxation from an unstable state.[1] A typical experiment concerning relaxation close to marginality in an optical bistable device is as follows.[1–4] The system is originally in a state of low transmission determined by a small value of the incident intensity. If this control parameter is now changed to a value close to the one associated with the end point of the lower branch of the hysteresis cycle the system will eventually relax to a state of high transmission in the upper branch. The difficulty associated with the description of such a relaxation process is easy to understand: If the final value of β in (1.1) is $\beta<0$, relaxation occurs via an activation mechanism of escape through a barrier due to fluctuations. Strictly at $\beta=0$ fluctuations are also necessary to leave the state $x=0$. For $\beta>0$ the relaxation is possible deterministically but fluctuations will considerably speed the process for small β. The mean-field con-

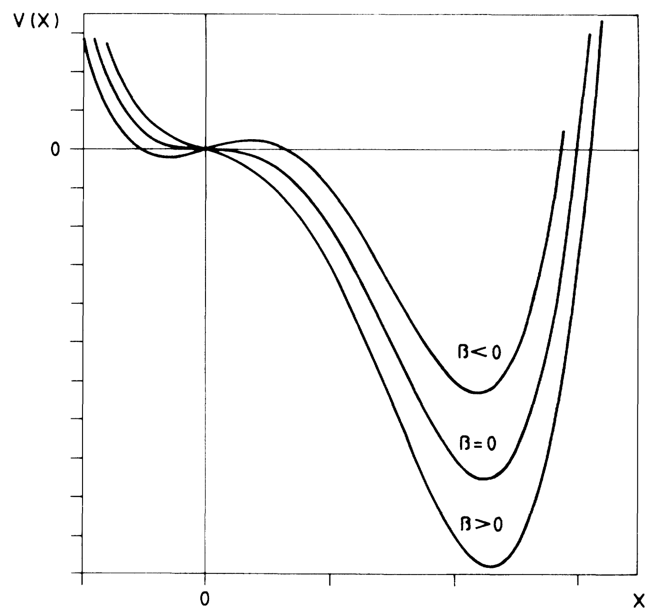

FIG. 1. Plot of the potential (1.1). $\beta<0$ corresponds to the inside of the hysteresis cycle with coexistence of two locally stable states separated by an unstable state. For $\beta>0$ a single stable state exists.

cept of critical slowing down associated with the end point of a hysteresis cycle indicates that the deterministic relaxation time diverges as $\beta \to 0$.[4(b)] Giving a unified description of the relaxation process for $\beta > 0$ and $\beta < 0$ requires the incorporation of very different mechanisms in the same scheme.

There are two alternative points of view to describe a relaxation process. A first one focuses directly on decay times[5] and the second one considers the transient evolution of statistical moments. Here we will mostly discuss decay times through the calculation of passage times statistics in analogy with the method followed by Arecchi[5] and co-workers to study the relaxation of a unstable state. The second approach is more directly connected with the phenomenon of transient bimodality[1] which we will not analyze here, although we will also characterize decay times by the evolution of statistical moments.

A good number of results for relaxation close to marginality exist in the literature, including experiments in illuminated passive nonlinear systems,[2(a)–2(c),3] analogic simulations,[2(a),2(b),2(d)] and numerical calculations[1] in models of optical bistability. In a characteristic experimental study[2(a)] the decay time as a function of noise intensity ϵ has been considered. Results largely deviate from the asymptotic dependence $t \approx \ln(1/\epsilon)$ well known for relaxation from an unstable state. The decay time as a function of the incident laser intensity has also been considered.[2(a),2(c),3(b)] More precise data for this dependence have been obtained through analogic simulations.[2(a),2(d)] These results give the change of behavior associated with the passage from an activation mechanism to a deterministic relaxation as discussed above. Another interesting aspect is the experimental finding[3] in a laser with saturable absorber of the simple dependence of the standard deviation ΔT of the passage-time distribution with the mean passage time T_1. Essentially, for small noise intensity parallel straight lines of ΔT versus T_1 for different noise intensities seem to occur.

In spite of the number of results and their similarity for different systems and models there does not seem to exist a clear unified theoretical understanding of them. Motivated by these results we address here this problem. Our aim is to find simple formulas of general validity for the statistics of the decay times. We are especially interested in describing the crossover involved in the change of mechanism of relaxation from $\beta > 0$ to $\beta < 0$ and also in finding model-independent features and possible universal laws describing the relaxation close to marginality. Our strategy for this purpose is to calculate with a simple model which captures the essential ingredients of marginality and to compare these results with a standard model of optical bistability. Our simple model is

$$\dot{x} = -V'(x) + \mu(t) , \tag{1.2}$$

where $\mu(t)$ is a Gaussian white noise of zero mean and correlation

$$\langle \mu(t)\mu(s) \rangle = 2\epsilon\delta(t-s) . \tag{1.3}$$

The potential $V(x)$ is a modified version of (1.1). Since we are only interested in the stages of evolution in which $x(t)$ leaves a state close to marginality, the saturation terms are not essential and we take

$$V(x) = -ax^3 - \beta x . \tag{1.4}$$

The standard model for purely absortive OB (Ref. 6) is

$$\dot{q} = Y - q - \frac{2Cq}{1+q^2} + \mu(t) , \tag{1.5}$$

where y is the amplitude of the incident field, normalized to the square of the saturation intensity, q is the normalized amplitude of the transmitted field, and C is the bistability parameter. A hysteresis cycle exists for $C > 4$. An expansion of (1.5) for q close to the marginal state reproduces (1.4) with $\beta = Y - Y_M$, Y_M being the up-switching threshold.[7]

Our main finding for a characteristic relaxation time is a simple formula which for small noise intensity is universal in the sense that it is independent of details of the model and valid for a large range of parameter values. It interpolates between Kramers time for activated decay and a deterministic relaxation time. It indicates that the characteristic time scales with $\epsilon^{-1/3}$. The relaxation time is given by a universal scaling function of the parameter $k = (\beta/a)(a/\epsilon)^{2/3}$ which measures deviation from marginality. For small k, a simple linear function of k determines the relaxation time. The scaling form found here for the relaxation time is a useful guide to reinterpret available experimental data for different β and ϵ. We also obtain a scaling form for the variance of the first-passage-time distribution from which a linear dependence of ΔT versus T_1 is found close to marginality with a slope independent of ϵ.

The paper is organized as follows: In Sec. II we discuss in general several alternative ways of characterizing the time scale associated with a decay process. A decay time characterized as a mean passage time is calculated in Sec. III and compared with simulation results. Section IV is devoted to the analysis of the variance of the passage-time distribution.

II. THEORETICAL FRAMEWORK

We will outline now three different alternatives to get the dominant time scale of the decay of a system governed by the model equations (1.2) and (1.5). The first method is the well known first-passage-time (FPT) technique. For a stochastic process one can define the interval of time that the process takes to reach for the first time a prescribed value x_F if it started at an initial value x_0. This interval of time is also a stochastic quantity whose mean value T_1 is the mean first-passage time (MFPT). Higher moments, T_n, can also be defined. The standard[8] theory of stochastic processes, when the noise $\mu(t)$ in (1.1) is a Gaussian white process, gives us the first moment and the variance[9] of the FPT distribution

$$T_1=\frac{1}{\epsilon}\int_{x_0}^{x_F}dx_1\, e^{V(x_1)/\epsilon}\int_{x_R}^{x_1}dx_2 e^{-V(x_2)/\epsilon} , \tag{2.1}$$

$$\Delta T^2\equiv T_2-T_1^2 ,=\frac{4}{\epsilon^2}\int_{x_0}^{x_F}dx_1\int_{x_R}^{x_1}dx_2\int_{x_R}^{x_2}dx_3\int_{x_R}^{x_3}dx_y \exp\{[V(x_1)+V(x_2)-V(x_3)-V(x_4)]/\epsilon\} , \tag{2.2}$$

where x_0 is the initial condition. These results correspond to a reflecting barrier placed at $x_R<x_0$ and an absorbing one at the final value x_F.

The second alternative comes from the analysis of the dynamical evolution of averaged quantities $f(x)$ defined by

$$\langle f(x(t))\rangle=\int_a^b dx\, f(x)P(x,t) , \tag{2.3}$$

where (a,b) is the domain of $x(t)$ and $P(x,t)$ its probability distribution at time t. Examples of these quantities are the statistical moments $\langle x^n(t)\rangle$. These quantities, understood as functions of t, define the analog of the FPT moments as

$$\langle t^n\rangle_f=\frac{\int_0^\infty t^n[\langle f(x(t))\rangle-\langle f\rangle_{\rm st}]dt}{\int_0^\infty[\langle f(x(t))\rangle-\langle f\rangle_{\rm st}]dt} , \tag{2.4}$$

where $\langle\ \rangle_{\rm st}$ is the average with the steady-state probability density $P_{\rm st}(x)$. It can also be defined the so-called nonlinear relaxation time (NLRT) as[10]

$$T_f\equiv\int_0^\infty\frac{\langle f(x(t))\rangle-\langle f\rangle_{\rm st}}{\langle f\rangle_0-\langle f\rangle_{\rm st}}dt , \tag{2.5}$$

where now $\langle\ \rangle_0$ is the average with the initial probability density $P(x,0)$. Following a method similar to that of Ref. 11 for the correlation function, the quantities (2.4) and (2.5) can be calculated exactly in terms of only $P_{\rm st}(x)$ and $P(x,0)$.[12] For an additive noise problem, the general solution for the NLRT associated to $f(x)$ and for the initial condition $P(x,0)=\delta(x-x_0)$ takes the form[12]

$$T_f=\frac{1}{f(x_0)-\langle f\rangle_{\rm st}}\frac{1}{\epsilon}\times\int_a^b P_{\rm st}^{-1}(x)\left[\int_a^x[f(x')-\langle f\rangle_{\rm st}]P_{\rm st}(x')dx'\right]\times\left[\theta(x-x_0)-\int_a^x P_{\rm st}(x')dx'\right]dx . \tag{2.6}$$

The NLRT defines a characteristic time of the process under study when there is a well-defined time scale, in which case it will give the same information as the MFPT.[12]

A third alternative to analyze similar dynamical information starts with the definition of the switching-time distribution[1(b)]

$$U_F(t)\equiv\frac{d}{dt}\int_{x_F}^b dx\, P(x,t) . \tag{2.7}$$

This distribution is related to the probability current $J(x,t)$ associated with the Fokker-Plank equation obeyed by $P(x,t)$

$$\frac{\partial}{\partial t}P(x,t)=-\frac{\partial}{\partial x}J(x,t) , \tag{2.8a}$$

$$J(x,t)=-V'(x)P(x,t)-\epsilon\frac{\partial}{\partial x}P(x,t) . \tag{2.8b}$$

In fact, $U_F(t)$ is equal to the probability current at the point x_F, $U_F(t)=J(x_F,t)$. Both the FPT and the switching-time distributions refer to the number of realizations which cross the threshold value x_F per unit time. The only difference is that the FPT problem removes the realizations when they reach the point x_F. In other case instead, they are not removed, so that a realization which has crossed the threshold can return and cross it in the opposite direction. The probability current $J(x_F,t)$ is the balance of the fluxes in both directions. As far as the return flux can be neglected, the two points of view are equivalent. In our case this equivalence holds until times of the order of the typical time to reach x_F from the absolute minimum of the potential, which is expected to be much greater than the time scale of the decay of the marginal state.

In the context of the definition (2.4) one can consider a characteristic time associated with the drift velocity $v(x)\equiv-V'(x)$. The averaged drift $\langle v(x(t))\rangle$ is just the velocity of the first moment

$$\langle v(x(t))\rangle=\frac{d}{dt}\langle x(t)\rangle . \tag{2.9}$$

It can be seen that the averaged drift if equal to the total-probability flux, so that in terms of the probability current it is given by

$$\langle v(x(t))\rangle=\int_a^b dx\, J(x,t) . \tag{2.10}$$

Actually the transient probability density in the marginal problem has two well-defined peaks,[1] so the velocity of the first moment accounts for the number of switches between the marginal and stable state per unit time. In fact, the dominant contribution to the integral (2.10) comes from the intermediate region, where $J(x_F,t)$ is essentially independent of x_F (except for times of the order of the deterministic time to leave the region). The averaged drift is thus similar to $J(x_F,t)$. As a consecuence, if we normalize the FPT distribution, the switching-time distributions, and the averaged drift as a function of t to a unit area, they have to be essentially equivalent in a wide range of intermediate times. The times are around the typical time scale of the decay of the marginal state. Furthermore the quantity $\langle v(x(t))\rangle$ allows us to connect the MFPT and the NLRT by means of the general result[12(b)]

$$\langle t\rangle_{v(x)}\equiv\frac{\int_0^\infty t\langle v(x(t))\rangle dt}{\int_0^\infty\langle v(x(t))\rangle dt}=T_x , \tag{2.11}$$

where T_x stands for the NLRT of the first moment and it is given by (2.5) with $f(x)=x$. Hence, since the normalized averaged drift is equivalent to the FPT distribution, T_x, $\langle t\rangle_v(x)$, and the MFPT have to be essentially equal.

The equivalence of the NLRT and the MFPT for the relaxation from marginality is explicitly shown below. These two quantities are calculated in Sec. III for our prototype equations (1.2)–(1.4) and compared with numerical simulation of (1.5).

The model defined by (1.2) and (1.4) does not have saturation term and consequently no stationary solution exists. In the study of the NLRT we will then introduce a reflecting barrier at the intermediate point $x_R'=R$, which plays the role of the threshold value x_F of the FPT problem. In the following we will call R indistinctly the position of the reflecting barrier x_R' (for NLRT calculations) and the absorbing barrier x_F (for FPT calculations).

We note that in this paper we restrict ourselves to relaxation triggered by additive white noise. It is not expected that multiplicative noise terms significantly change the relevant time scales. In fact, the main features of experiments[2] which involve multiplicative noise are well described by our results.

III. DECAY TIMES

We now address the explicit calculation of decay times for relaxation from marginality using the general formulas (2.1) and (2.6) for the MFPT and the NLRT for x. The calculation is based on the universal model (1.2)–(1.4) and results are compared with simulations for the model (1.5) of optical bistability with $x_0=-q_M$ ($q_0=0$), $q_F=10$, and $R=q_F-q_M$.[7] We will consider separately the strict case of marginality ($\beta=0$) and the situation close to marginality $\beta\neq 0$ which permits the study of passage from $\beta<0$ to $\beta>0$.

A. $\beta=0$ (purely marginal case)

This case was studied in Refs. 9 and 13 with the initial condition at the marginal point $x_0=0$. The asymptotic evaluation of (2.1) in the limit of small intensity of the noise gives for the MFPT

$$T_1(0\to R)=A_0(a^2\epsilon)^{-1/3}+C(R)+\Theta(\epsilon/aR^3)\ , \qquad (3.1)$$

where the constant $A_0=1.594\,850\,2\ldots$ is obtained by numerical integration of (2.1) and $C(R)=-1/(3aR)$. Equation (3.1) shows that the T_1 scales with noise intensity $\epsilon^{-1/3}$.[9,13,14] This is a universal property of a cubic marginal state. The next contribution is a constant, $C(R)$, and it is model dependent. Since $C(R)$ does not depend on ϵ and has dimensions of time it must be related to an intrinsic deterministic time of the model.

From the experimental point of view it is hard to be strictly at marginality $\beta=0$ and to fix the initial condition just in the marginal point. As a first step to the more normal physical situation we consider relaxation at $\beta=0$ with an initial condition at $x_0<0$ (for $x_0>0$ the relaxation is mostly governed by the deterministic forces). In this case the asymptotic evaluation of the MFPT from (2.1), for $|x_0|>(\epsilon/a)^{1/3}$, gives

$$T_1(x_0\to R)=B_0(a^2\epsilon)^{-1/3}+C(x_0,R)+\Theta\left[\frac{\epsilon}{aR^3},\frac{\epsilon}{a|x_0|^3}\right]\ , \qquad (3.2)$$

where $C(x_0,R)=(3ax_0)^{-1}+C(R)$ and $B_0=\Gamma(\frac{1}{3})^2/3$. The numerical factor B_0 includes now the time necessary to approach the marginal point from $x_0<0$. As in the previous case (3.1) the next contribution is a model-dependent constant $C(x_0,R)$.

In order to check the general ideas discussed in Sec. II we now consider the nonlinear relaxation time for $\langle x(t)\rangle$, with $P(x,0)=\delta(x-x_0)$. From the general expression (2.6) for $x_0=0$ we obtain

$$T_x(0)=A_0(a^2\epsilon)^{-1/3}+C(R)+\Theta\left[\frac{\epsilon}{aR^3}\right]\ . \qquad (3.3)$$

We observe that (3.3) has the same structure as the result (3.1) for the MFPT, and both quantities have the same dominant term. This is also true for the relaxation of other moments. The constant $C(R)$, which we know is model dependent, is also the same as in (3.1) but it can differ for higher-order moments.

If the initial condition is located at $x_0<0$ and $|x_0|\gg(\epsilon/a)^{1/3}$ we obtain

$$T_x(x_0)=\frac{R}{R+|x_0|}\left[B_0(a^2\epsilon)^{-1/3}+C_1(x_0,R)+\frac{B_1}{2aR}+\Theta\left[\frac{\epsilon}{aR^3},\frac{\epsilon}{a|x_0|^3}\right]\right]\ , \qquad (3.4)$$

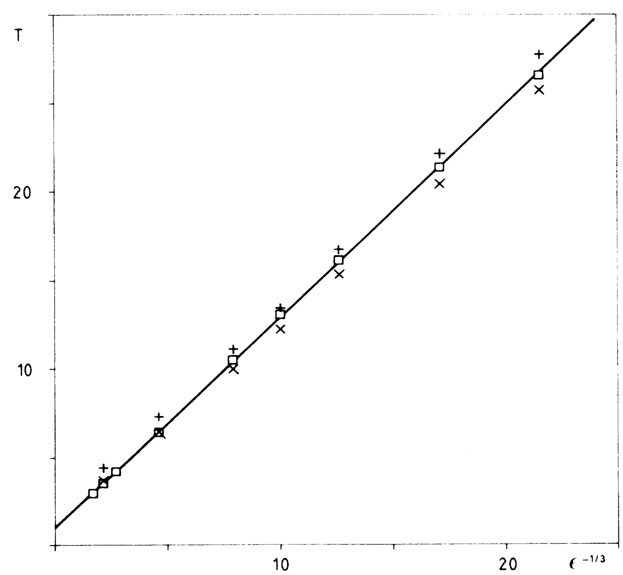

FIG. 2. Different characteristic times vs $\epsilon^{-1/3}$. The squares correspond to the MFPT; pulses correspond to the NLRT associated with the first moment and the crosses to the NLRT of the second moment. All the points correspond to the simulation of the model (1.5). The solid line is the fit of the MFPT with the theoretical slope. Values taken for the parameters in (3.1) are $x_0=-1.054$, $R=10$, $a=1.82$, corresponding to (1.5) with $C=20$, $q_0=0$.

where $C_1(x_0,R)=C(x_0,R)-(3aR)^{-1}\ln(R/|x_0|)$. The result is also essentially the same. The differences appear in the constant and in the prefactor. This last is an artifact of the definition which comes from the normalization procedure. It is, in some sense, reminiscent of the global character of the NLRT. In conclusion, (3.1)–(3.4) show that the MFPT and the NLRT convey the same basic information on the decay time associated with the relaxation process. The same thing is true for relaxation from an unstable state.[12]

To check the general validity of (3.2) we compare in Fig. 2 this prediction with simulation results for MFPT and NLRT obtained for the model (1.5). The ordinate at the origin $C'(q_0,q_F)$, which depends on the particularities of the model, can be fitted from the simulation data or calculated analytically.[15] We observe that the asymptotic law is valid for a wide range of values of ϵ with very similar results for the different decay times considered. Small differences appear in the ordinate at the origin and in the slope due to the prefactors coming from the definition of the NLRT.

B. $\beta\neq 0$

We now consider the case $\beta\neq 0$, and $x_0<0$ which describes the typical experimental situation mentioned in the introduction. We will consider the situation where β is small. The region $\beta>0$ corresponds to most of the experimental results. Here we will also study the region $\beta<0$ and we will establish the connection between both regions. The asymptotic evaluation of the MFPT (2.1) for small ϵ and β, with $|x_0|\gg(\epsilon/a)^{1/3}$ and $|x_0|\gg(\beta/a)^{1/2}$, gives

$$T_1(x_0\to R)=\phi(k)(a^2\epsilon)^{-1/3}+C(x_0,R)+\Theta\left[\frac{\epsilon}{aR^3},\frac{\epsilon}{a|x_0|^3},\frac{\epsilon}{aR^2},\frac{\beta}{a|x_0|^2}\right], \tag{3.5}$$

where the universal function $\phi(k)$ is given by

$$\phi(k)=\left[\frac{\pi}{2}\right]^{1/2}\int_0^\infty dz\frac{1}{\sqrt{z}}e^{-(z^3/4)-kz}=\sum_{n=0}^{\infty}(-1)^n\frac{B_n}{n!}k^n, \tag{3.6}$$

with

$$B_n=\frac{1}{3}\left[\frac{\pi}{3}\right]^{1/2}2^{2n+1/2}\Gamma\left[\frac{2n+1}{6}\right], \tag{3.7}$$

and a new important parameter k appears

$$k=(\beta/a)(a/\epsilon)^{2/3}. \tag{3.8}$$

The second contribution in (3.5) is the same constant that in (3.2) and therefore independent of a, ϵ, and β.[15] In the limits $x_0\to\infty$, $R\to\infty$, the MFPT is exactly given by

$$T_1(-\infty\to+\infty)=\phi(k)(a^2\epsilon)^{-1/3} \tag{3.9}$$

for all β and ϵ (for this model).

Equation (3.5) indicates that T_1 still scales with $\epsilon^{-1/3}$ for $\beta\neq 0$. This parameter k measures the distance to the marginality ($k=0$). The system will display marginal behavior provided $|k|$ is small enough. This is an important criterion in the experiments. In fact, this agrees with the experimental results of Lange.[2] There one can observe how a system which is not in a strictly marginal state displays marginal behavior when the values of ϵ, β, and a are such that k is small enough.

The function $\phi(k)$ is analytic for all values of k and it can also be expressed in terms of hypergeometric functions.[16] The validity of keeping one or two terms in the series is given by the smallness of k. The structure of the series explains the different behavior of T for $\beta>$ or <0. For $\beta<0$ all the terms in the series are positive and a large value of T is obtained. In fact, for $\beta<0$ there is a potential barrier of height $(\frac{4}{3})(|\beta|^3/3a)^{1/2}$. When $|k|\gg 1$, very far from marginality, and $\beta<0$ we are in the high-barrier limit in which the dominant contribution of (3.6) is

$$\phi(k)\approx(\pi^2/3|k|)^{1/2}\exp(4|k/3|^{3/2}), \tag{3.10}$$

which reproduces the Kramers escape time

$$T_1\approx(\pi^2/3|\beta|a)^{1/2}\exp(4|k/3|^{3/2}). \tag{3.11}$$

In the low barrier limit ($|k|\ll 1$, marginality), it is interesting to consider the situation in which the initial condition x_0 is at the minimum of the potential, $x_0=-(\beta/3a)^{1/2}$. We obtain, from (2.1),

$$T_1(x_0\to R)=(a^2\epsilon)^{-1/3}\left[A_0+\Gamma\left[\frac{1}{3}\right]\left[\frac{|k|}{27}\right]^{1/2}+\theta(k)\right]+C(R)+\Theta\left[\frac{\epsilon}{aR^3},\frac{\beta}{aR^2}\right]. \tag{3.12}$$

The second contribution in (3.12) gives a dependence of the form $(1/a)(a/\epsilon)^{2/3}|\beta/a|^{1/2}$ also found in Ref. 17 as a first correction to the marginal case.

For $\beta>0$, (3.6) is an alternating series giving a small value of T which as $\epsilon\to 0$, tends to the deterministic value

$$T_{\mathrm{det}}(x_0,R)=-\int_{x_0}^{R}\frac{dx}{V'(x)}. \tag{3.13}$$

The study of the NLRT for the same situation gives similar results are expected. Explicitly, we obtain

$$T_x(x_0)=\frac{R}{R+|x_0|}\left\{\phi(k)(a^2\epsilon)^{-1/3}+C_1(x_0,R)-\frac{1}{2aR}\phi'(k)\right\}+\theta\left[\frac{\epsilon}{aR^3},\frac{\epsilon}{a|x_0|^3},\frac{\beta}{aR^2},\frac{\beta}{a|x_0|^2}\right]. \tag{3.14}$$

Except for the prefactor, the dominant contribution is the same as that for the MFPT (3.5). Differences appear in the next-order contributions.

General consequences of (3.5) and its universal properties are displayed in Figs. 3 and 4 where again the prediction (3.5) is compared with simulations of the model (1.5). In Fig. 3 one can see the different behavior of the MFPT for distinct values of β. For $\beta<0$, the MFPT diverges as the noise intensity goes to zero, since the system has to

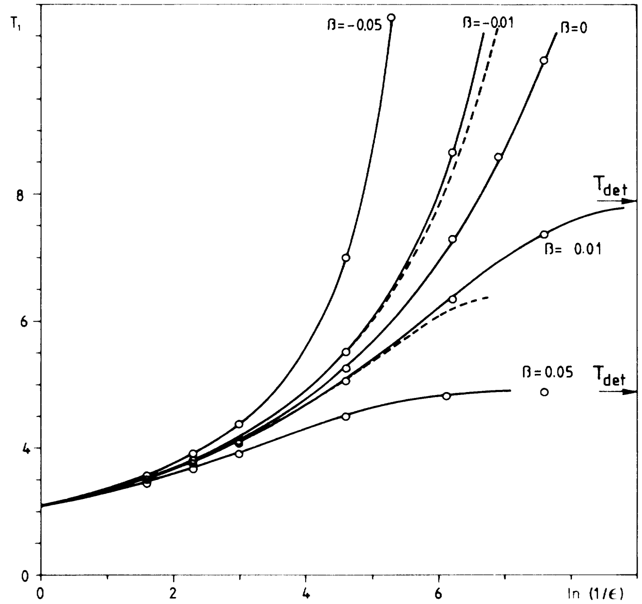

FIG. 3. MFPT vs $\ln(1/\epsilon)$ for different values of β. The circles correspond to the numerical simulation of (1.5). Solid lines are the theoretical prediction (3.5) with the constant $C'(q_0,q_F)$ determined in Fig. 2. Dashed lines are the first-order approximation in k for $\phi(k)$. Same parameter values as in Fig. 2.

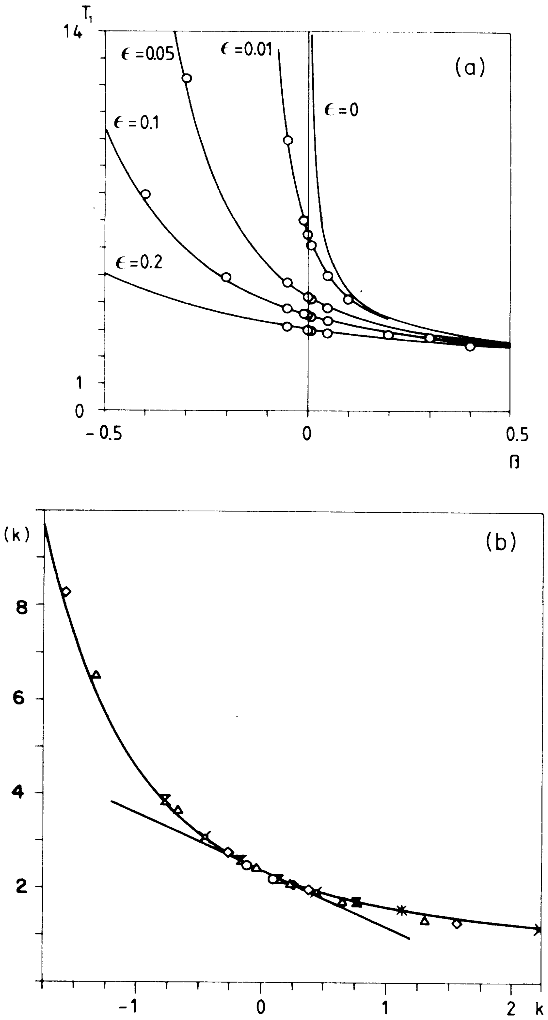

FIG. 4. MFPT vs β for different values of ϵ. Solid lines correspond to the theoretical prediction of the universal model (1.2)–(1.4). Circles correspond to the simulation of the model (1.5). Same parameter values as in Figs. 2 and 3. (b) $[T_1-C'(q_0,q_F)](a^2\epsilon)^{1/3}$ vs k obtained from simulations for different values of β ($\bigcirc=0.2$; $\triangle=0.1$; $\diamondsuit=0.05$; $X=0.01$; $\square=0.002$; $*=0.0005$). The curve corresponds to the function $\phi(k)$ and the straight line is its first approximation in k.

cross a barrier. For $\beta>0$ we have curves which saturate to the corresponding deterministic time for $\epsilon\rightarrow 0$. These S-shaped curves are in agreement with recent experimental results.[2(a)] At the same time they discard the straight-line fitting of Refs. 1 and 2(a), which is valid for the decay from unstable states but not close to marginality. In the region of $\epsilon\approx 1$ all the curves coalesce together as one would expect for noise-dominated dynamics. The broad domain of validity of (3.5) with respect to noise intensity and the validity of keeping only the first approximation to $\phi(k)$ are also shown in Fig. 3. A remarkable point is the excellent agreement between the points obtained from the simulation[18] of the model (1.5) of Bonifacio and Lugiato,[6] and the solid curves, which are calculated for the universal model (1.2)–(1.4) [with the constant $C'(q_0,q_F)$ corresponding to (1.5)]. This reinforces the idea of universality which is more clearly displayed in Figs. 4.

Fig. 4(a) shows the MFPT versus β for different values of ϵ. In the case of $\epsilon=0$ the MFPT diverges for $\beta=0$ (critical slowing down). For $\epsilon\neq 0$ the asymptotic behavior for $\beta<0$ is the exponential of the Kramers law (3.10) and (3.11). The change of behavior from $\beta<0$ to $\beta>0$ indicates the change from relaxation via activation by fluctuations to relaxation via deterministic dynamics. Such behavior of T as a function of β is also manifest in the experimental results of Refs. 2(a), 2(c), 2(d), and 3. The similarity of the curves in Fig. 4(a) for different ϵ suggests that some kind of scaling law could occur. This is content in our formula (3.5) which is made explicit in Fig. 4(b). The MFPT minus the corresponding constant $C'(q_0,q_F)$ scaled by $\epsilon^{1/3}$ is plotted versus k. All these curves in Fig. 4(a) coalesce then into a single curve with all the point lying on this same curve which is precisely the universal scaling function $\phi(k)$ of Eq. (3.5). It would be certainly interesting to look for this scaling form of the relaxation time in experiments of relaxation close to marginality.

IV. FIRST-PASSAGE-TIME VARIANCE

Up to now we have addressed the study of the time scale of the decay of a marginal state. Our next step is the characterization of the width of the FPT distribution by means of its variance $\Delta T^2\equiv T_2-T_1^2$. For the purely marginal case ($\beta=0$) this quantity was also studied in Ref. 9. We consider separately the cases $\beta=0$ and $\beta\neq 0$.

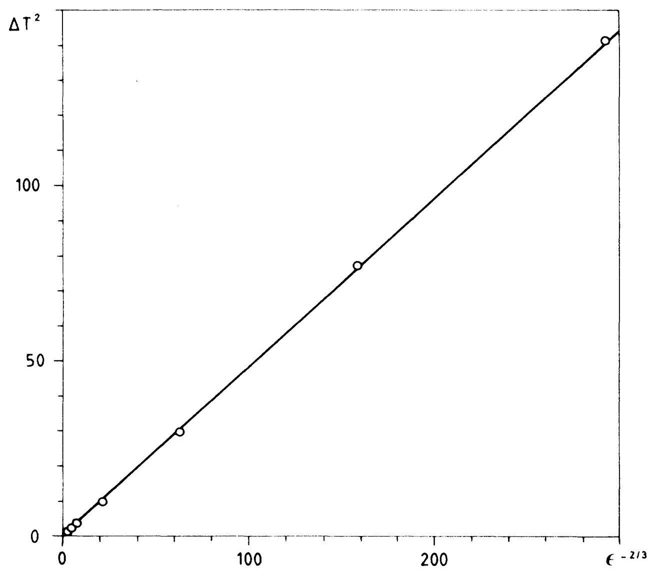

FIG. 5. Variance of the FPT distribution vs $\epsilon^{-2/3}$. The line is the fit with the theoretical slope (3.22) and the circles correspond to the simulation of (1.5).

A. $\beta=0$

For the initial condition $x_0=0$ the asymptotic evaluation of (2.2) for the universal model (1.2)–(1.4) gives

$$\Delta T^2=\tilde{A}_0(a^2\epsilon)^{-2/3}-\frac{2}{135}\frac{\epsilon}{a^3R^5}+\Theta\left[\frac{\epsilon^2}{a^2R^6}\right], \tag{4.1}$$

where now $\tilde{A}_0=1.747\ldots$. The first term in (4.1) is universal. The corrections to the asymptotic law given by this first term are model dependent. If $x_0<0$ and $|x_0|\gg(\epsilon/a)^{1/3}$ we obtain

$$\Delta T^2=\tilde{B}_0(a^2\epsilon)^{-2/3}-\frac{2\epsilon}{135a^3}\left[\frac{1}{|x_0|^5}+\frac{1}{R^5}\right]$$

$$+\Theta\left[\frac{\epsilon^2}{a^2R^6},\frac{\epsilon^2}{a^2|x_0|^6}\right], \tag{4.2}$$

where $\tilde{B}_0=\Gamma^4(\frac{1}{3})/27$. Once again only the first contribution is universal. It corresponds to the exact result when $x_0\to-\infty$ and $R\to\infty$, for this model.

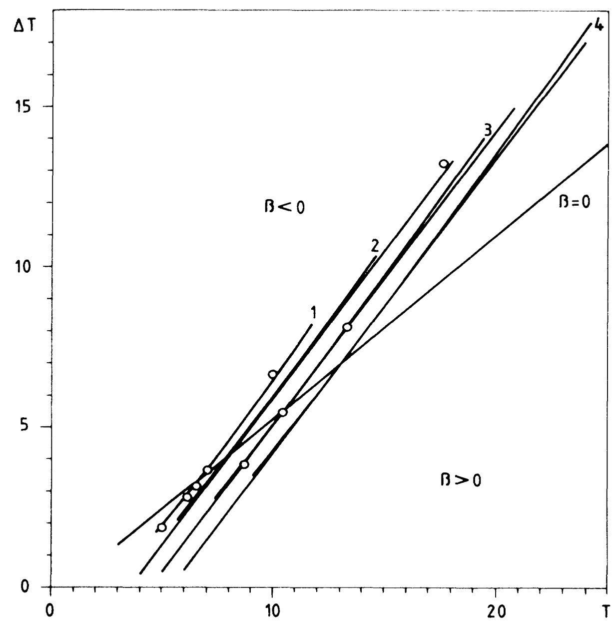

FIG. 6. First-passage-time variance vs the MFPT close to marginality ($\beta=0$) for different ϵ. Lines 1, 2, 3, and 4 correspond to $\epsilon=0.01$, 0.005, 0.002, and 0.001, respectively. Straight lines are given by (3.8) and the slightly curved lines include the entire dependence on k of $\phi(k)$. Points are simulation results from (1.5). Parameter values are the same as in Figs. 2 and 3.

In (4.1) and (4.2) no constant term independent of ϵ appears, since ΔT must vanish for $\epsilon\to0$. In Fig. 5 we have plotted the first-passage-time variance obtained from simulation of the Bonifacio-Lugiato model.[6] The straight line corresponds to fit the results with the predicted slope (4.2).

B. $\beta\neq0$

In this case we have

$$\Delta T^2=\tilde{\phi}(k)(a^2\epsilon)^{-2/3}+\Theta\left[\frac{\epsilon}{aR^3},\frac{\epsilon}{a|x_0|^3}\right], \tag{4.3}$$

where

$$\tilde{\phi}(k)=\sum_{n=1}^{\infty}(-1)^n k^n\tilde{B}n/n! \tag{4.4}$$

and

$$\tilde{B}_n=4\int_{-\infty}^{\infty}dx_1\int_{-\infty}^{x_1}dx_2\int_{-\infty}^{x_2}dx_3\int_{-\infty}^{x_3}dx_4(x_1+x_2-x_3-x_4)^n e^{x_4^3+x_3^3-x_2^3-x_1^3}. \tag{4.5}$$

Equation (4.3) indicates that ΔT^2 scales with $\epsilon^{-2/3}$. Up to first order in k the results (3.5) and (4.3) become

$$T_1=(a^2\epsilon)^{-1/3}(B_0-B_1k)+C(x_0,R)\ , \tag{4.6}$$

$$\Delta T^2=(a^2\epsilon)^{-2/3}(\widetilde{B}_0-\widetilde{B}_1k)\ . \tag{4.7}$$

Eliminating now k in these two equations we can get a linear dependence between ΔT and T_1 in a lowest-order approximation

$$\Delta T\approx\alpha+\sigma T_1\ , \tag{4.8}$$

where

$$\alpha=-0.376(a^2\epsilon)^{-1/3}-0.92C(x_0,R) \tag{4.9}$$

and the slope σ is independent of ϵ

$$\sigma=\frac{\widetilde{B}_1}{2B_1\sqrt{\widetilde{B}_0}}=0.92\ . \tag{4.10}$$

In Fig. 6 we have plotted the standard deviation of the FPT distribution ΔT versus the MFPT for different noise intensities. This makes explicit the linear dependence implied by (4.8) close to marginality. The points correspond to the simulation of the model (1.5). We can conclude that deviations of the exact curves from the linear approximation are not very important around the marginality region where that linear dependence is confirmed also by simulation, occurring with a slope which does not depend on ϵ. Such collection of parallel lines was suggested by the experimental observation of Arimondo *et al.*[3] in optical bistability of a CO_2 laser with saturable absorver close to marginality. The approximation (4.8) and the result given by the complete function $\phi(k)$ are shown.

ACKNOWLEDGMENTS

We acknowledge financial support from Dirección General de Investigación Científica y Técnica (Spain) (Projects PR-84-0361, PB-86-0534, and AE-87-0035). Helpful discussions with E. Arimondo and L. A. Lugiato are acknowledged.

[1](a) G. Broggi and L. A. Lugiato, Phys. Rev. A **29**, 2949 (1984); (b) G. Broggi, L. A. Lugiato, and A. Colombo, *ibid.* **32**, 2803 (1985).

[2](a) R. Deserno, R. Kumme, P. Mitschke, W. Lange, and J. Mlynek, SPIE **700**, 83 (1986); W. Lange, *Noise in Nonlinear Dynamical Systems,* edited by P. Moss and P. McClintock, (Cambridge University Press, Cambridge, 1988), Chap. 27; (b) W. Lange, F. Mitschke, R. Deserno, and J. Mlynek, Phys. Rev. A **32**, 1271 (1985); (c) W. Lange, *Instabilities and Chaos in Quantum Optics II,* Vol. 177 of *NATO Advanced Study Institute, Series B: Physics,* edited by N. B. Abraham, F. T. Arecchi, and L. A. Lugiato (Plenum, New York, 1988); (d) F. Mitschke, R. Deserno, J. Mlynek, and Lange , IEEE **QE-81**, 1435 (1985).

[3](a) E. Arimondo, D. Dangoise, L. Fronzoni, O. Incani, and N. K. Rahman (unpublished); (b) E. Arimondo, C. Gabanini, E. Menchi, and B. Zambon, SPIE **667**, 234 (1986).

[4](a) A different situation concerns the possibility of placing the system in the unstable branch of the hysteresis cycle. See, for example, J. Y. Bigot, A. Dunois, and P. Mandel, Phys. Lett. A **123**, 123 (1987). We will also not discuss the situation in which the incident intensity is continuously varied sweeping across the end point of the hysteresis cycle; (b) P. Mandel, in *Optical Bistability, Instability and Optical Computing,* edited by H-Y. Zhang and K. K. Lee (World Scientific, Singapore, 1988).

[5]F. T. Arecchi and A. Politi, Phys. Lett. **77A**, 312 (1980); F. T. Arecchi, A. Politi, and L. Ulivi, *ibid.* **87A**, 333 (1982).

[6](a) L. A. Lugiato, *Progress in Optics XXI,* edited by E. Wolf (North-Holland, Amsterdam, 1984); (b) R. Bonifacio and L. A. Lugiato, Phys. Rev. A **18**, 1129 (1978).

[7]For $C=20$ (Ref. 1) we have $Y_M=21.0264$. The marginal state occurs for $Y=Y_M$ and $q=q_M=1.0543$. This corresponds in our simplified model to $a=2.8201$ and $x=q-q_M$.

[8]C. W. Gardiner, *Handbook of Stochastic Methods for Physics, Chemistry and Natural Sciences,* Vol. 13 of *Springer Series in Synergetics,* edited by H. Haken (Springer, Berlin, 1983).

[9]F. T. Arecchi, A. Politi, and L. Ulivi, Nuovo Cimento **71B**, 119 (1982). We note a numerical discrepancy in the constant A_0 in Eq. (3.1).

[10]K. Binder, Phys. Rev. B **8**, 3423 (1973).

[11]P. Jung and H. Risken, Z. Phys. B **59**, 469 (1985).

[12](a) J. I. Jiménez-Aquino, J. Casademunt, and J. M. Sancho, Phys. Lett. A (to be published); (b) J. Casademunt, J. I. Jimenez-Aquino, and J. M. Sancho (unpublished).

[13]B. Caroli, C. Caroli, and B. Roulet, Physica **101A**, 581 (1980).

[14]In the case of higher-order marginality simple dimensional arguments show that T_1 scales as $\epsilon^{-(n-2)/n}$, where n is the dominant power of the potential. [J. M. Sancho, in *Synergetics, Order and Chaos,* edited by M. G. Velarde (World Scientific, Singapore, in press)].

[15]In fact, the constant $C'(q_0,q_F)$ of a given model will be given in a general case [see Eq. (3.5)] by the difference $T_1(x_0\rightarrow R)-\phi(k)(a^2\epsilon)^{1/3}$ in the simultaneous limits $\epsilon\rightarrow 0$ and $\beta\rightarrow 0$. For $\beta>0$, deterministic trajectories exist, so the difference between $C'(q_0,q_F)$ and the constant corresponding to a reference model [for instance, (1.4)] will be given by the difference between the respective deterministic times (finite quantities), in the limit $\beta\rightarrow 0^+$. This calculation can be performed directly in the limit $\beta=0$ because, although both deterministic times diverge, the difference is finite and easy to calculate using (3.13).

[16]For $\beta>0$ the series is alternate so it converges rapidly and few terms are usually necessary. For $\beta<0$, it is monotonic and the convergence is slower.

[17]G. S. Agarwal and S. R. Shenoy, Phys. Rev. A **23**, 2719 (1981).

[18]J. M. Sancho, M. San Miguel, S. L. Katz, and J. D. Gunton, Phys. Rev. A **26**, 1589 (1982).